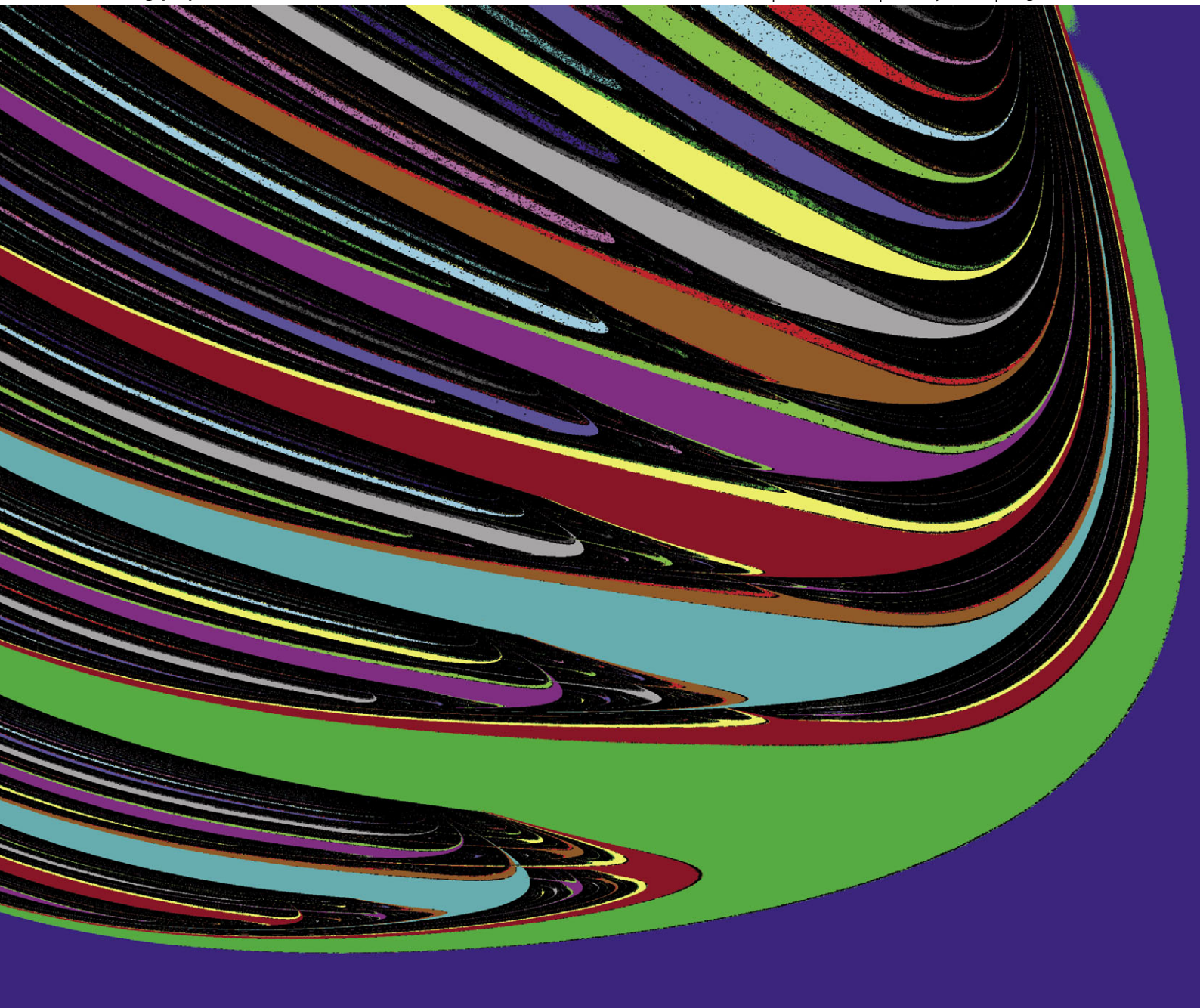


# PCCP

Physical Chemistry Chemical Physics

[www.rsc.org/pccp](http://www.rsc.org/pccp)

Volume 13 | Number 26 | 14 July 2011 | Pages 12101–12336



ISSN 1463-9076

**COVER ARTICLE**

Freire and Gallas  
Stern–Brocot trees in the periodicity  
of mixed-mode oscillations

**HOT ARTICLE**

Geiger *et al.*  
On molecular chirality within naturally  
occurring secondary organic aerosol  
particles from the central Amazon  
Basin



1463-9076(2011)13:26;1-U

Cite this: *Phys. Chem. Chem. Phys.*, 2011, **13**, 12191–12198

www.rsc.org/pccp

PAPER

## Stern–Brocot trees in the periodicity of mixed-mode oscillations

Joana G. Freire<sup>ab</sup> and Jason A. C. Gallas<sup>\*abc</sup>

Received 3rd December 2010, Accepted 13th January 2011

DOI: 10.1039/c0cp02776f

We investigate the distribution of mixed-mode oscillations in the control parameter space for two paradigmatic chemical models: a three-variable fourteen-parameter model of the Belousov–Zhabotinsky reaction and a three-variable four-parameter autocatalator. For both systems, several high-resolution phase diagrams show that the number of spikes of their mixed-mode oscillations emerges consistently organized in a surprising and unexpected symmetrical way, forming Stern–Brocot trees. The Stern–Brocot tree is more general and contains the Farey tree as a subtree. We conjecture the Stern–Brocot hierarchical organization to be the archetypal skeleton underlying several systems displaying mixed-mode oscillations.

### 1. Introduction

Mixed-mode oscillations (MMOs) are complex oscillatory patterns consisting of trains of small amplitude oscillations followed by large excursions of relaxation type. During the last 30 years or so, MMOs were observed profusely in experiments and models of prototypic chemical systems.<sup>1–24</sup> In the literature, MMOs were also called *alternating periodic-chaotic* sequences.<sup>14,15</sup> For a recent survey about the properties, prospection and use of MMOs in several fields see ref. 25.

Although MMOs were already investigated abundantly, they were analyzed most frequently by considering the dynamics observed along a single or a few scattered one-parameter sections of parameter spaces that are normally of very high dimensions. Sometimes, a few bifurcation curves were obtained using numerical continuation techniques. It seems then natural to ask if restricted sections of the high-dimensional parameter spaces are sufficient for an unambiguous characterization of MMO cascades. Here we show that the periodicity of MMO cascades still harbors unsuspected and far-reaching organizational features.

The aim of this paper is to present a detailed investigation of the unfolding of MMO cascades as observed when *two parameters are tuned finely* in the control space of two representative examples of chemical dynamics, namely the Belousov–Zhabotinsky reaction<sup>4,5</sup> and in one of the commonly exploited model schemes based on isothermal autocatalysis.<sup>6,7</sup> This is done by numerically computing high-resolution planar phase diagrams for these systems.

The main result reported here is the discovery of a surprisingly new hierarchical organization for MMOs in parameter space of both examples mentioned. In contrast to what is presently known, in both models we find MMOs to emerge organized in perfect agreement with the so-called Stern–Brocot tree,<sup>26,27</sup> not according to the familiar Farey tree.<sup>28</sup> The Stern–Brocot trees are more general than Farey trees and include them as subtrees.<sup>29,30</sup> Stern–Brocot trees may be recognized contemplating the unfolding of oscillations in several two-parameter sections of the control parameter space. Before proceeding, we remark that we also found Stern–Brocot trees in other popular models of MMOs. Here, however, we wish to focus on the aforementioned pair of representative models, namely a realistic Belousov–Zhabotinsky proxy and the autocatalator.

Our motivation for this work arises from the fact that the period-adding sequences commonly found in MMOs systems display a striking resemblance with aspects of sequences observed recently in rather distinct scenarios connected with certain “periodicity hubs”.<sup>31–34</sup> When projected in planar phase diagrams, multidimensional hub manifolds produce remarkable networks of points responsible for *organizing* very regularly the dynamics around quite wide portions of the parameter space.<sup>34</sup> For us, systems displaying MMOs are particularly attractive to investigate and probe details associated with the nature of certain intricate reinjection mechanisms, homoclinic or not, causing periodicity hubs<sup>33,34</sup> and of reinjections arising in multiple-timescale systems. Such mechanisms need to be investigated because they play important roles in the generation of a radically distinct class of stability spirals than those presently known, a class for which not even a local adequate mathematical framework is available at present.<sup>35</sup>

In the next section we review briefly a realistic model of the Belousov–Zhabotinsky reaction and introduce what we call “isospike diagrams” illustrating how the number of spikes of

<sup>a</sup> Instituto de Física, Universidade Federal do Rio Grande do Sul, 91501-970 Porto Alegre, Brazil. E-mail: jgallas@if.ufrgs.br

<sup>b</sup> Departamento de Matemática, Centro de Estruturas Lineares e Combinatórias, Universidade de Lisboa, Lisboa, Portugal

<sup>c</sup> Departamento de Física, Universidade Federal da Paraíba, 58051-970 João Pessoa, Brazil

periodic oscillations auto-organizes in five distinct sections of their control parameter space. Section 3 describes the Stern–Brocot organization arguing that this is the hierarchical organization of the MMOs in the Belousov–Zhabotinsky reaction. Section 4 presents results for the autocatalator model providing independent corroboration of the Stern–Brocot organization. Although isospike diagrams of both models display the same hierarchical Stern–Brocot structure, they are easier to be recognized in the autocatalator, in the sense that autocatalator requires fewer phase diagrams to display the organization. Finally, Section 5 summarizes our conclusions.

## 2. Isospike diagrams for a realistic BZ model

The Belousov–Zhabotinsky reaction is a classical dynamical system for which several mathematical models have been developed over the years with an ever increasing degree of reality.<sup>16–20</sup> Here, we consider a model suggested by Györgyi and Field<sup>4</sup> that contains 14 parameters that may be tuned to produce rich dynamical scenarios.<sup>5</sup> It is governed by three differential equations:

$$\begin{aligned} \frac{dx}{d\tau} = T_0 \left\{ -k_1 H Y_0 x \tilde{y} + k_2 A H^2 \frac{Y_0}{X_0} \tilde{y} - 2k_3 X_0 x^2 \right. \\ \left. + 0.5k_4 A^{0.5} H^{1.5} X_0^{-0.5} (C - Z_0 z) x^{0.5} \right. \\ \left. - 0.5k_5 Z_0 x z - k_f v \right\}, \end{aligned} \quad (1)$$

$$\begin{aligned} \frac{dz}{d\tau} = T_0 \left\{ k_4 A^{0.5} H^{1.5} X_0^{0.5} \left( \frac{C}{Z_0} - z \right) x^{0.5} - k_5 X_0 x z \right. \\ \left. - \alpha k_6 V_0 z v - \beta k_7 M z - k_f z \right\}, \end{aligned} \quad (2)$$

$$\begin{aligned} \frac{dv}{d\tau} = T_0 \left\{ 2k_1 H X_0 \frac{Y_0}{V_0} x \tilde{y} + k_2 A H^2 \frac{Y_0}{V_0} \tilde{y} \right. \\ \left. + k_3 \frac{X_0^2}{V_0} x^2 - \alpha k_6 Z_0 z v - k_f v \right\}, \end{aligned} \quad (3)$$

where we abbreviated<sup>5</sup>

$$x \equiv \frac{X}{X_0}, y \equiv \frac{Y}{Y_0}, z \equiv \frac{Z}{Z_0}, v \equiv \frac{V}{V_0}, \tau \equiv \frac{t}{T_0}, \quad (4)$$

$$X \equiv [\text{HBrO}_2], A \equiv [\text{BrO}_3^-],$$

$$Y \equiv [\text{Br}^-], C \equiv [\text{Ce(III)}] + [\text{Ce(IV)}],$$

$$Z \equiv [\text{Ce(IV)}], H \equiv [\text{H}^+],$$

$$V \equiv [\text{BrMA}], M \equiv [\text{CH}_2(\text{COOH})_2],$$

and where  $X_0 = k_2 A H^2 / k_5$ ,  $Y_0 = 4X_0$ ,

$$Z_0 = \frac{CA}{40M}, V_0 = 4 \frac{AHC}{M^2}, T_0 = \frac{1}{10k_2 AHC}, \quad (5)$$

$$\tilde{y} = \frac{\alpha k_6 Z_0 V_0 z v}{(k_1 H X_0 x + k_2 A H^2 + k_f) Y_0}. \quad (6)$$

**Table 1** Numerical values of rate constants and parameters fixed in our simulations, taken from ref. 4, in the same units

$k_1 = 4 \times 10^6$	$k_2 = 2.0$
$k_3 = 3 \times 10^3$	$k_4 = 55.2$
$k_5 = 7 \times 10^3$	$K_6 = 0.09$
$k_7 = 0.23$	$k_f = 3.9 \times 10^{-4}$
$A = 0.1$	$C = 8.33 \times 10^{-4}$
$H = 0.26$	$M = 0.25$
$\alpha = 666.7$	$\beta = 0.3478$

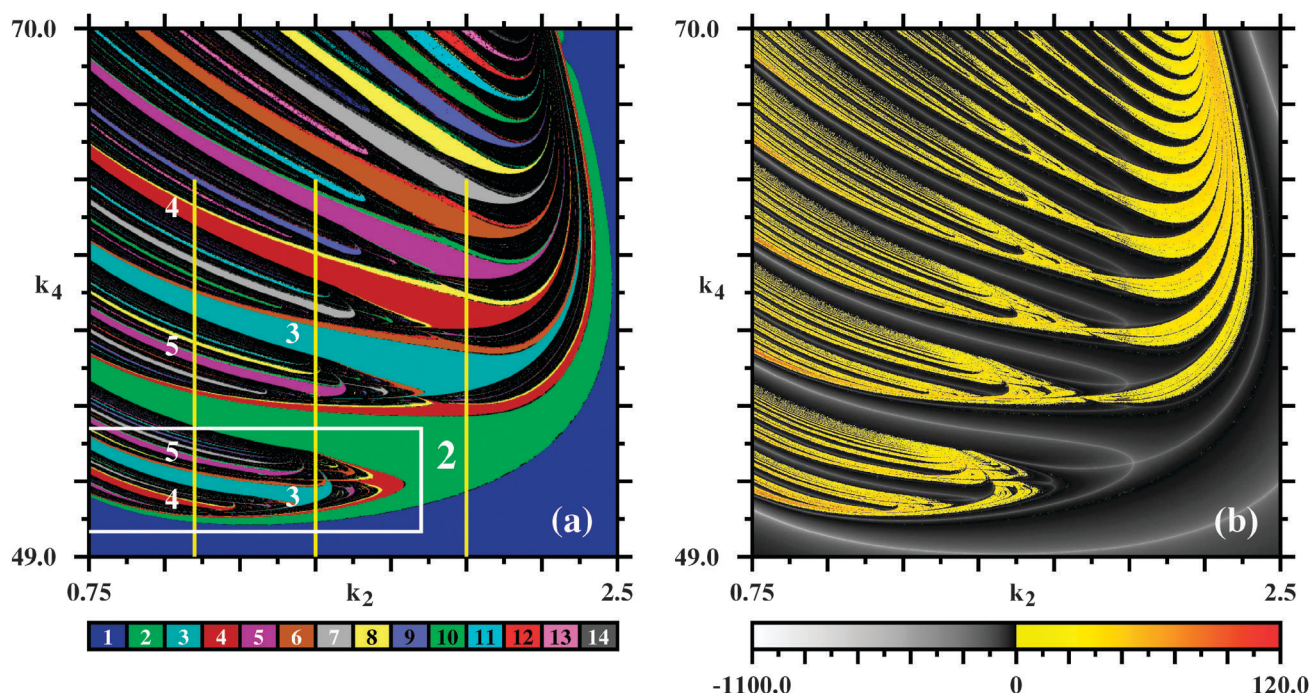
The quantities  $\alpha$  and  $\beta$  are historical artifacts and have no chemical significance.<sup>5</sup> All parameters appearing in the equations above are collected in Table 1, along with their basic numerical values. Further details about this model are available in the literature.<sup>4,5</sup>

Fig. 1 presents a pair of phase diagrams that we computed for eqn (1)–(3). In both diagrams, the parameter region shown was divided into a mesh of  $1200 \times 1200$  equally spaced values. For each parameter pair, we integrated eqn (1)–(3) using a standard fourth-order Runge–Kutta algorithm with fixed time-step  $h = 2 \times 10^{-6}$ . The first  $2.5 \times 10^6$  steps were discarded as transient. During the next  $2.5 \times 10^6$  steps we searched for the local maxima of the variable displaying the largest number of spikes within a period,  $x$  for the BZ reaction. The number of spikes was then plotted in what we call *isospike diagrams*, with the help of colors, as indicated in the diagrams. As it is known, the number of spikes of each independent variable is not uniformly equal.<sup>31</sup>

Computations were always started from the lowest value of  $k_2$  from the arbitrary initial condition  $(x_0, z_0, v_0) = (0.046, 0.898, 0.846)$  and continued by *following the attractor*, namely, by using the values of  $x, z, v$  obtained at the end of one integration at a given  $k_2$  to start a new calculation after incrementing  $k_2$  infinitesimally. This is a standard way of generating bifurcation and Lyapunov diagrams, and the rationale behind it is that, generically, basins of attraction do not change significantly upon slight changes of parameters, thereby ensuring a relatively smooth unfolding of the quantity being investigated as parameters evolve. Lyapunov exponents were computed in a similar way, as described in ref. 5.

Fig. 1a shows an isospike diagram, discriminating with colors parameter domains characterized by periodic oscillations having an identical number of spikes within a period. Such diagram is a sort of generalized isoperiodic diagram,<sup>36–38</sup> useful for visualizing the organization of periodic phases. Fig. 1a displays the 14 lowest periods using the 14 colors indicated by the colorbar, recycling them “mod 14” for higher periods. Black is used to represent parameters leading to non-periodic oscillations, *i.e.* to chaos. This same scale is used in similar figures below where, additionally, white is used to mark fixed-points (*i.e.* non-oscillatory solutions).

In Fig. 1a it is possible to recognize a dense succession of curved stripes indicating that periodic oscillations with an ever increasing number of spikes exist symmetrically on both sides of the green stripe (which marks parameters leading to periodic oscillations with two spikes in a period). On both sides of the green 2-spoke phase one may recognize the unfolding of the doubling cascade ending in chaos (black). Next comes a large region characterized by three spikes, together with its doubling cascade, ending once again in chaos (black).



**Fig. 1** Phase diagrams for the Belousov–Zhabotinsky reaction. (a) Isospike diagram emphasizing periodic phases. Chaotic phases are shown in black. The white box indicates the location of the lower “armpit” of the 2-spike phase. The three vertical lines indicate the parameters investigated in the bifurcation diagrams shown in Fig. 2. Colors and numbers mark the number of peaks in a period of  $x$ , as indicated by the colorbar. Colors are used “mod 14”, *i.e.* we recycle the same colors for higher periods. Period-adding cascades are easily recognizable along a continuum of one-parameter, codimension one, lines. (b) Lyapunov phase diagram emphasizing chaotic phases. Although generated in distinct ways, the dynamical phases predicted by both diagrams agree with each other. Each panel displays results from the phase-space analysis of the dynamics for  $1200^2 = 1.44 \times 10^6$  individual parameter points.

Fig. 1b displays a Lyapunov phase diagram<sup>34,39–41</sup> corresponding to the panel shown in Fig. 1a. The emphasis in the Lyapunov phase diagram is on enhancing the intricate and large chaotic phase, *i.e.* making chaos more easily visible. Colors denote parameters leading to chaos, *i.e.* positive exponents, while darker shadings mark periodicity, as indicated by the color bar. The color scale for the Lyapunov exponents is linear on both sides of zero but not uniform from negative to positive extrema. Note that although Fig. 1a and b are obtained using two very distinct algorithms, they both agree: the boundaries between chaotic and periodic regions delimited by Lyapunov exponents coincide with the boundaries obtained by counting spikes.

Fig. 1a manifests a clear structural organization of the isospike phases and it is natural to ask about how this ordering further develops for higher periods. The large blue phase in Fig. 1a corresponds to 1-spike oscillations. When moving to the left from this 1-spike phase one meets the green 2-spike phase corresponding to a period doubling of the 1-spike oscillations. Moving further to the left one sees that the 2-spike phase develops two distinct “armpits”, *i.e.* two phases characterized by period doubling cascades that accumulate in a chaotic phase, represented in black in Fig. 1a [in yellow in Fig. 1b]. The white box in Fig. 1a indicates the location of the lower armpit of the 2-spike phase. Although each chaotic phase contains a myriad of smaller isospike phases, the *largest periodic phases* embedded in the chaotic phases of the 2-spike armpits are a symmetric pair of 3-spike phases, as indicated by

the labels “3” in the figure. Each one of these 3-spike phases develops its own symmetric pair of armpits. To see how this multiplication process develops is difficult in the scale of Fig. 1a. However, the structure may be recognized resorting to several magnifications and bifurcation diagrams of specific portions of the phase diagram (not shown here).

In this way we recognize that the general picture underlying the hierarchical process at hand is the emergence of an infinite cascade of armpit pairs appearing in a definite order which, albeit strongly distorted in the figures, display a mirror symmetry with respect to the central 2-spike green domain. This central domain seems to organize the whole structure as periods grow without bound.

Fig. 2 presents bifurcation diagrams showing the evolution of the variable  $x$  (the normalized concentration  $X = [\text{HBrO}_2]$ ) along the three vertical lines shown in Fig. 1a. The bifurcation diagrams contain numbers to help identify the location of some of the major windows of periodic behavior and to facilitate comparison with the planar windows depicted in Fig. 1a. The bifurcation diagrams emphasize the fact that it is very hard to grasp the hierarchical ordering of the MMOs based solely on a few isolated diagrams.

Fig. 3 shows four additional parameter sections of the 14-dimensional parameter space of the Belousov–Zhabotinsky reaction. As it is clear from this figure, all sections display the same hierarchical organization found for Fig. 1a. It is important to realize that the parameters used in all figures here do not reflect abstract choices but, instead, are

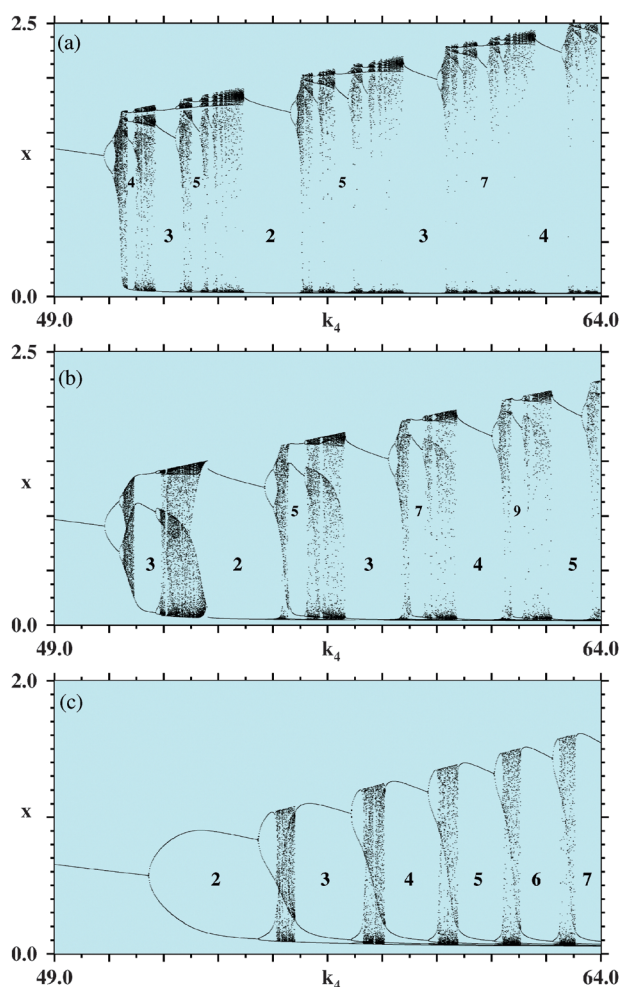


**Fig. 2** Bifurcation diagrams showing the evolution of  $x$  (i.e. of the normalized concentration  $X = [\text{HBrO}_2]$ ) along the three vertical lines shown in Fig. 1a. Numbers indicate the number of spikes characterizing the windows containing them. The Belousov–Zhabotinsky model has an accumulation of spikes close to zero as  $k_4$  increases. Bifurcations along (a)  $k_2 = 1.1$ ; (b)  $k_2 = 1.5$ ; (c)  $k_2 = 2.0$ .

parameters derived from real experiments.<sup>4</sup> This is why our cuts produce rather asymmetric trees. We believe to be possible to optimize parameters so as to generate much more symmetric parameter sections. Such search, however, is expected to be computationally very time-consuming and will not be pursued at this point.

In Fig. 4 we summarize schematically the first few levels of the hierarchical organization of MMOs observed in the five sections of the parameter space of the Belousov–Zhabotinsky reaction, shown in Fig. 1 and 3. To emphasize the symmetry of the hierarchical structure, in Fig. 4 we compensated shifts and shear normally present in phase diagrams. The fine structure of the hierarchical development of MMOs is of course rather complex but Fig. 4 certainly captures its *Leitmotiv*.

### 3. The tree of Stern and Brocot

The correlation between the MMOs observed progressively in parameter space is traditionally investigated by establishing a one-to-one correspondence between these oscillations and an

ordered set of rational numbers. To do this it is usual to start by first establishing a taxonomy for MMOs by introducing symbols like  $L^s$ , where  $L$  and  $s$  refer, respectively, to the number of “large” and “small” amplitude excursions recorded in the time evolution of one of its variables.

A well-known ordering of rationals is generated by assigning to a given pair  $p/q$  and  $p'/q'$  of rationals an intermediary “mediant” rational  $(p + p')/(q + q')$ . Since the number of spikes in a period is defined by an integer, not by a rational number, we consider “derived trees” formed by simply summing  $p$  and  $q$  of familiar trees used in number theory to represent sequences of rationals. Fig. 5 compares the sequences of rationals generated by Stern–Brocot<sup>29</sup> and by Farey<sup>28</sup> sequences with the *sum trees* derived from them by simply adding numerator and denominator of the rationals.

As it is clear from Fig. 5, the spike ordering of the MMOs in Fig. 1a does not correspond to the one generated by the Farey tree but it is in perfect agreement with the integers in the Stern–Brocot sum tree. This “good” tree was devised independently in 1858 by Moritz Stern<sup>26</sup> and in 1861 by Achille Brocot.<sup>27</sup> Stern was a German mathematician and Brocot a French clockmaker. The latter used this tree to design systems of gears with a gear ratio close to some desired value by finding a ratio of numbers near that value. The Stern–Brocot and Farey trees are generated by the same arithmetic principle. However, Stern–Brocot trees are more general than Farey trees and include them as subtrees.<sup>29,30</sup>

The Stern–Brocot sequence differs from the Farey sequence in two basic ways:<sup>29</sup> it eventually includes all positive rationals, not just the rationals within the interval  $[0,1]$ , and at the  $n$ th step all mediants are included, not only the ones with denominator equal to  $n$ . The Farey sequence of order  $n$  may be found by an in-order traversal of the left subtree of the Stern–Brocot tree, backtracking whenever a number with denominator greater than  $n$  is reached. “*But we had better not discuss the Farey series any further, because the entire Stern–Brocot tree turns out to be even more interesting.*”<sup>29</sup>

Two factors are important to identify the Stern–Brocot tree: first, one needs to sweep finely two parameters simultaneously and, second, the tree is made visible by the isospike diagrams introduced here. We find the total number of spikes to be a more reliable indicator than the standard large–small  $L^s$  labeling and the associated “winding numbers”  $W = s/(L + s)$  derived from such labeling. These quantities turn out to be rather ambiguous when tuning two parameters on a finely spaced mesh. For instance, the attribution of the labels  $1^0$  and  $0^1$  is ambiguous from the outset as also is the set of multiple labels which are possible in sequences of spikes with comparable amplitudes evolving as parameters are changed slightly, due to difficulties in distinguishing “large” from “small”. Furthermore, the Farey tree has been frequently identified in the literature on the basis of “devil staircases” constructed with the aforementioned winding numbers, despite ambiguities and despite the fact that  $L^s$  and the infinite sequence  $(nL)^{(ms)}$  for  $n = 2,3,\dots$  share identical winding numbers.

Farey trees have been identified in earlier work on the basis of the analysis of a *single* chemical variable. It is important to realize that although phase diagrams obtained by using just one of the dynamical variables are easier to obtain and

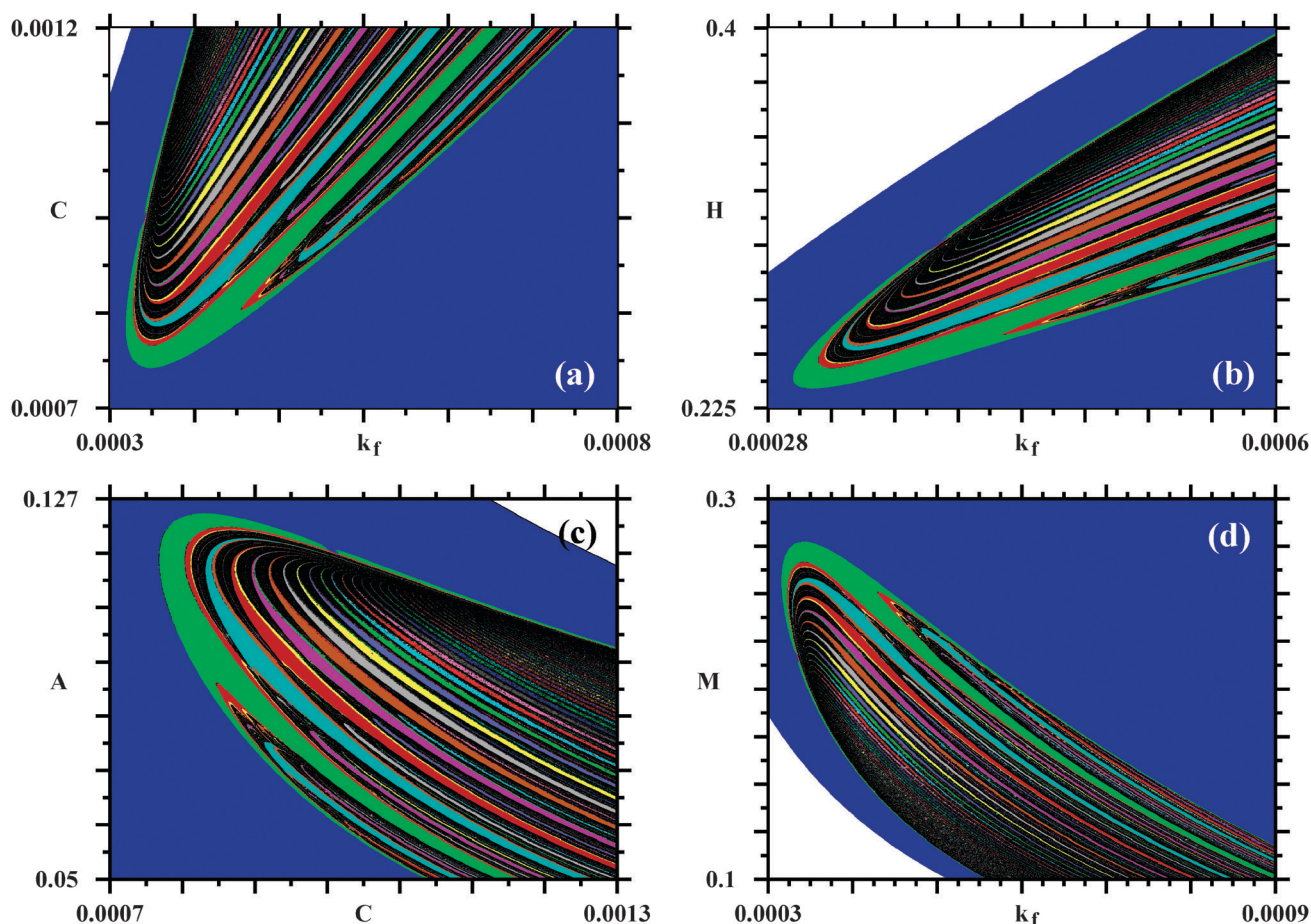


**Fig. 3** Examples of Stern–Brocot trees observed in four additional sections of the 14-dimensional parameter space of the Belousov–Zhabotinsky reaction. The relative invariance of the diagrams seems to imply the existence of a highly symmetric hyper-manifold in parameter space. White regions represent fixed-point (non-oscillating) solutions. The white–blue boundaries are lines of Hopf bifurcations. The “fountains of chaos” described in ref. 5 are here identified as manifestations of the Stern–Brocot order defined in Fig. 4 and 5 below. Each panel displays results from the phase-space analysis of the dynamics for  $1200^2 = 1.44 \times 10^6$  individual parameter points.

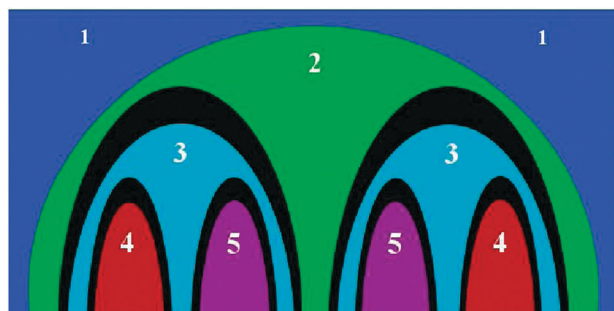


**Fig. 4** Schematic representation of the first stages of the hierarchical unfolding of isospike cascades observed in MMOs. The black regions between isospike phases represent chaotic phases of non-homogeneous chaos,<sup>34</sup> reached after cascades of period doubling bifurcations. The “armpits” of the main 2-spoke phase contain a pair of 3-spoke phases, each one containing their own pair of armpits with isospike phases, with this hierarchical organization repeating *ad infinitum*, showing a mirror symmetry with respect to the central 2-spoke domain. As shown in Fig. 5 below, the sequence of periods here corresponds to that generated by the Stern–Brocot tree.

generally reliable, the final diagram might depend on the choice of the variable. For instance, identical isospike diagrams are

obtained when counting spikes from either  $x(t)$  or  $z(t)$  in eqn (1) and (2). The oscillations of  $v(t)$  in eqn (3) are less representative than the ones from the former two variables. This is so because the number of spikes of individual variables governing dynamical systems evolves independently from each other.<sup>31</sup> When constructing isospike diagrams, we always use one of the variables that displays the greatest temporal variation, *i.e.* the greatest number of spikes within a period. In any case, dependencies may be eliminated by using *vector* quantities defined by taking into consideration all components governing the flow, a superfluous step for our present purposes. Be it as it may, eventual dependencies need to be ascertained on a case-by-case basis by studying all dynamical variables involved.

We emphasize that isospike diagrams may be used equally well to discriminate between a Stern–Brocot and a Farey tree. For any given system, its specific tree may be read directly from the organization and the sequencing seen in the computed isospike phases. Note, however, that isospike diagrams provide no information about the relative magnitudes or about the sequence of oscillations within a period. Isospike diagrams work as useful complements to the traditional tools, like, *e.g.*, time-evolution plots and bifurcation diagrams, being certainly not a substitute for any of them.

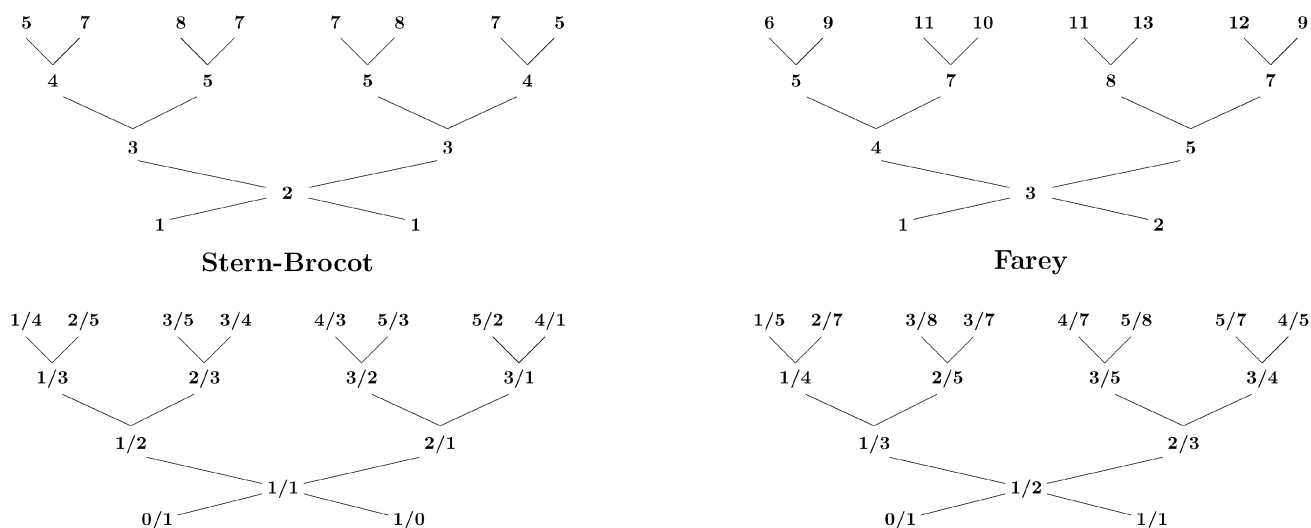


**Fig. 5** Top row: tree of periods obtained by summing numerator and denominator of the fractions in the Stern–Brocot and Farey trees. Bottom row: schematic representation of the Stern–Brocot and the Farey trees. The sequence of periods derived from the Stern–Brocot tree reproduces the hierarchy of the periodic phases in Fig. 1a and 3. The arithmetic process responsible for the growth of both trees is the same.

#### 4. Stern–Brocot tree in the autocatalator model

To check the generality of the Stern–Brocot spike-ordering we performed an additional experiment, investigating the ordering of MMOs for a paradigmatic autocatalator defined by the equations<sup>6,7</sup>

$$\frac{dA}{dt} = \mu(C + \kappa) - A(B^2 + 1), \quad (7)$$

$$\sigma \frac{dB}{dt} = A(B^2 + 1) - B, \quad (8)$$

$$\delta \frac{dC}{dt} = B - C, \quad (9)$$

where  $A, B, C$  are dimensionless concentrations, and  $\mu, \kappa, \sigma, \delta$  are freely tunable control parameters.

Fig. 6 presents phase diagrams demonstrating clearly that the hierarchical structure of MMOs for the autocatalator coincides with the one found earlier in Fig. 1 and 3 for the Belousov–Zhabotinsky reaction. Even the strong “lateral compression” seen in both diagrams looks identical.

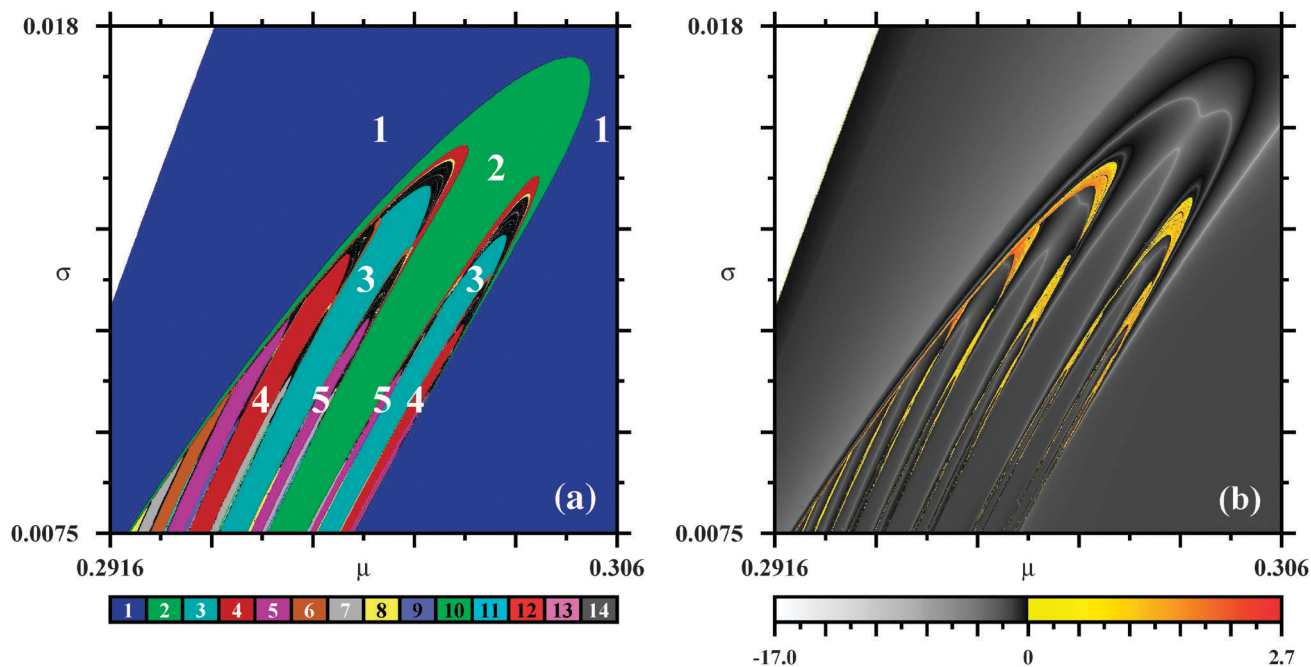


**Fig. 6** (a) Isospike diagram for the autocatalator. (b) The corresponding Lyapunov phase diagram. These figures complement Fig. 7 of Petrov *et al.*<sup>7</sup> White spines seen in the Lyapunov diagram are continuous-time generalized loci analogous to discrete-time *superstable loci*.<sup>37</sup> The white–blue and white–black boundaries in the upper left corners are Hopf bifurcation lines. Here  $k = 2.5$  and  $\delta = 1$ . Each panel displays results obtained from the individual phase-space analysis of  $1200^2$  parameter points.

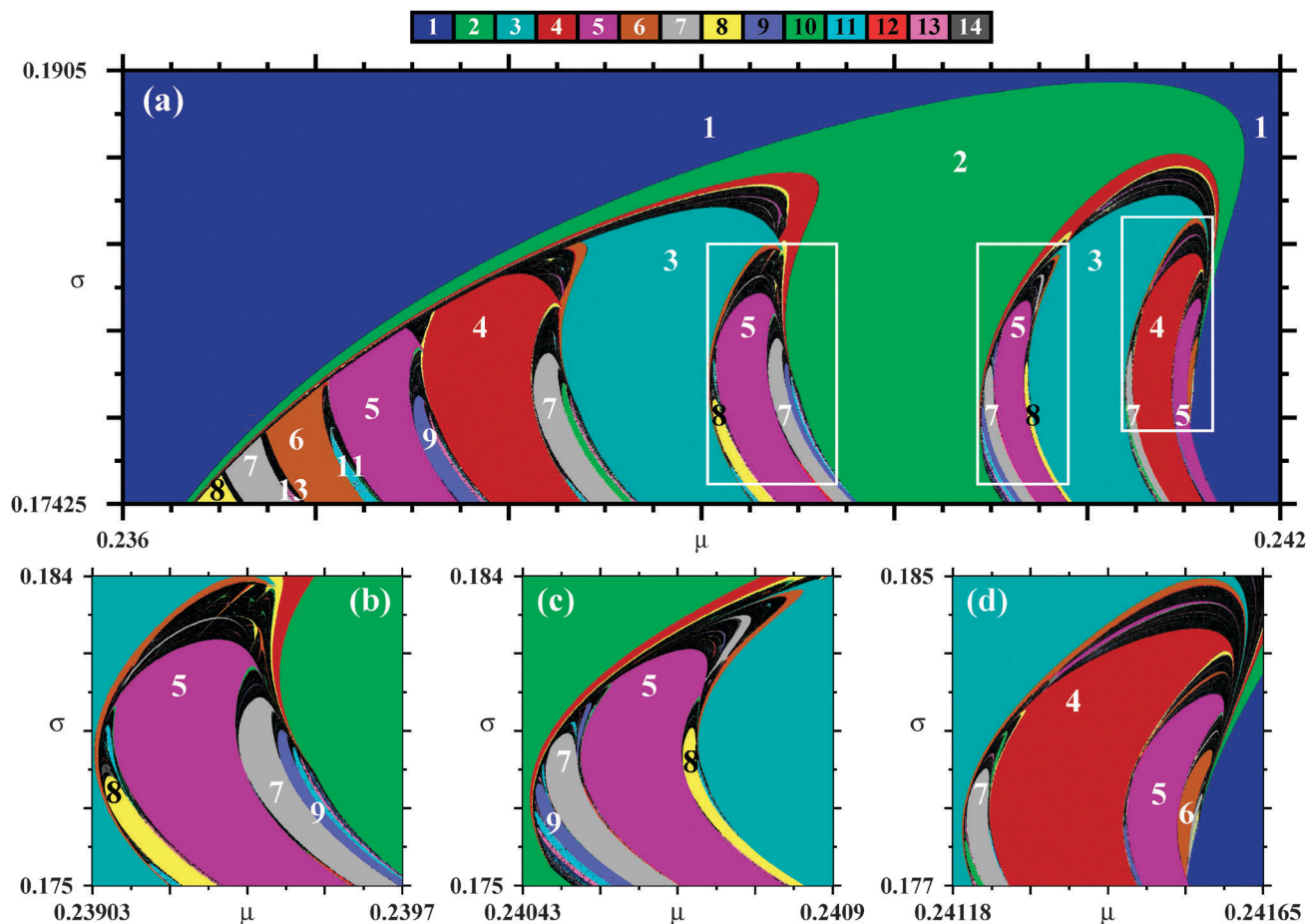


**Fig. 7** Top: isospike diagram displaying the Stern–Brocot organization as observed in the autocatalator after rotation in parameter space. Colors and numbers display the number of peaks in a period of  $B$ . Some regions are too small to be identified in this scale but become visible under magnification. Resolution:  $2400 \times 1200$  parameter points. Bottom: enlargement of the white boxes, showing details of the Stern–Brocot tree. Each of the three panels displays results obtained from the individual phase-space analysis of  $1200^2$  parameter points.

To minimize the lateral compression and to better visualize the unfolding of the isospike cascade, we recomputed Fig. 6a after suitably rotating the  $(\mu, \sigma)$  parameter plane by an angle  $\theta = \pi/5$  around the point  $(\mu_0, \sigma_0) = (0.0072, 0.00525)$  according to the transformation<sup>37</sup>

$$\mu' = \mu_0 + (\mu - \mu_0)\cos\theta - (\sigma - \sigma_0)\sin\theta, \quad (10)$$

$$\sigma' = \sigma_0 + (\mu - \mu_0)\sin\theta + (\sigma - \sigma_0)\cos\theta. \quad (11)$$

Isospike diagrams in the rotated framework are shown in Fig. 7 where, for simplicity, we drop primes from the transformed coordinates. This figure allows a more detailed view of the unfolding of the cascade, which is seen to also follow the Stern–Brocot order.

It is clear from the several phase diagrams presented here that the hierarchical structure found for the MMOs in the Belousov–Zhabotinsky reaction and in the autocatalator displays an excellent agreement. In fact, macroscopically both hierarchical structures observed may be considered as isomorphic to each other. A detailed report about MMOs observed in the autocatalator is being prepared and will be presented elsewhere.<sup>42</sup>

## 5. Conclusions

We performed a detailed study of the unfolding of cascades of mixed-mode oscillations for two prototypical chemical models by continuously recording changes in the number of spikes of their periodic oscillations when pairs of parameters are tuned simultaneously. In several sections of the parameter space, we found that the number of spikes emerges organized according to a regular tree of integers that may be easily derived from the Stern–Brocot tree, not from the much more familiar Farey tree. The Stern–Brocot trees are more general than Farey trees and include them as subtrees.<sup>29,30</sup>

The arithmetic process for generating Stern–Brocot and Farey trees is exactly the same. But the specific tree obtained shows sensitive dependence to the initial conditions. Alone, the arithmetic process does not discriminate Farey from Stern–Brocot order. In fact, since the “mediant” arithmetics of both trees is exactly the same, it is generally very hard to guess the right tree underlying cascades of oscillations based solely on isolated cuts of parameter space or on a few bifurcation diagrams displaying a limited number of windows.

We argued that the plain use of winding numbers based on large/small labeling might not be a reliable indicator to

discriminate Farey from Stern–Brocot order because such labeling cannot sensibly be defined generically. Since only the Farey tree is presently believed to have been sighted in devil’s staircases generated by MMOs, an enticing challenge now seems to be to sort out Stern–Brocot from Farey order in such cascades. We remark that sequences of rational numbers are easy to attribute to phenomena involving two distinct frequencies. But it looks rather arbitrary to use the non-unique concept of large/small peaks to emulate pairs of frequencies in phenomena where they are not naturally present or not quite justifiable.

The fact that the Stern–Brocot tree is clearly visible in so many distinct sections of the parameter space of the Belousov–Zhabotinsky model seems to imply the existence of an exceptionally symmetric manifold in its parameter space, a sort of “hyper-symmetrical onion” capable of displaying identical-looking sections when cut along several distinct directions, as exemplified by Fig. 1 and 3. The realistic Belousov–Zhabotinsky model considered here is governed by a set of fourteen parameters;<sup>4,5</sup> a nice and presumably time-consuming computational challenge now would be to try to locate the “symmetry center” of such onion, if any.

Although not yet reported, we have also identified the Stern–Brocot spike ordering to be equally present in a few additional standard models displaying MMOs.<sup>43</sup> Therefore, we believe the Stern–Brocot tree to hold great significance for the generic description of the hierarchical structure of complex oscillatory patterns routinely observed in chemical systems supporting mixed-mode oscillations, as evidenced by the phase diagrams shown above. In fact, our numerical investigations seem to suggest the Stern–Brocot tree to emerge by far more frequently than the nowadays so popular Farey tree: thus far we have been unable to find evidence of Farey trees in isospike diagrams computed for a dozen or so of the standard models known for displaying MMOs and purportedly containing Farey trees.

In conclusion, to the *abstract* application of Stern in number theory and the nice *practical* application devised originally by Brocot, this paper now adds another practical use for the Stern–Brocot tree: to describe and predict the regular and symmetrical unfolding and multiplication of spike cascades in mixed-mode oscillations, as indicated schematically in Fig. 4 and 5. We hope our work to motivate the experimental verification of Stern–Brocot order of MMOs in chemical oscillators and in other interesting systems.

JACG is grateful to R. Montandon, Buchs, Switzerland, and P. Ribenboim, Kingston, Canada, for providing a copy of Brocot’s delightful original paper<sup>27</sup> and for their kind interest in this work. JGF thanks for a Post-Doctoral fellowship from FCT, Portugal, grant SFRH/BPD/43608/2008, and IF-UFRGS for hospitality. JACG is supported by CNPq, Brazil, and by the US Air Force Office of Scientific Research, grant FA9550-07-1-0102. All computations were done in the computer clusters of CESUP-UFRGS.

## References

- J. Hudson, M. Hart and D. Marinko, *J. Chem. Phys.*, 1979, **71**, 1601.
- J. S. Turner, J. C. Roux, W. D. McCormick and H. L. Swinney, *Phys. Lett. A*, 1981, **85**, 9.
- P. Ibson and S. K. Scott, *J. Chem. Soc., Faraday Trans.*, 1990, **86**, 3695.
- L. Györgyi and R. J. Field, *Nature*, 1992, **355**, 808.
- J. G. Freire, R. J. Field and J. A. C. Gallas, *J. Chem. Phys.*, 2009, **131**, 044105.
- B. Peng, S. K. Scott and K. Showalter, *J. Phys. Chem.*, 1990, **94**, 5243.
- V. Petrov, S. K. Scott and K. Showalter, *J. Chem. Phys.*, 1992, **97**, 6191.
- K. Krischer, M. Eiswirth and G. Ertl, *J. Chem. Phys.*, 1992, **96**, 9161.
- K. Krischer, M. Lübke, M. Eiswirth, W. Wolf, J. L. Hudson and G. Ertl, *Phys. D*, 1993, **62**, 123.
- I. R. Epstein and K. Showalter, *J. Phys. Chem.*, 1996, **100**, 13132.
- N. Baba and K. Krischer, *Chaos*, 2008, **18**, 015103.
- K. Kovacs, M. Leda, V. K. Vanag and I. R. Epstein, *J. Phys. Chem. A*, 2009, **113**, 146.
- L. Yuan, Q. Gao, Y. Zhao, X. Tang and I. R. Epstein, *J. Phys. Chem. A*, 2010, **114**, 7014.
- For a survey see: H. L. Swinney, *Phys. D*, 1983, **7**, 3, and references therein.
- T. Braun, J. Lisboa and J. A. C. Gallas, *Phys. Rev. Lett.*, 1992, **68**, 2770, and references therein.
- I. R. Epstein and J. A. Pojman, *An Introduction to Nonlinear Chemical Dynamics: Oscillations, Waves, Patterns, and Chaos*, Oxford University Press, New York, 1998.
- R. J. Field and L. Györgyi, *Chaos in Chemistry and Biochemistry*, World Scientific, Singapore, 1993.
- P. Gray and S. K. Scott, *Chemical Oscillations and Instabilities*, Oxford Science Publications, New York, 1990.
- A. M. Zhabotinsky, *Scholarpedia*, 2007, **2**(9), 1435.
- L. Györgyi and R. J. Field, *J. Phys. Chem.*, 1991, **95**, 6594.
- R. Larter and C. G. Steinmetz, *Philos. Trans. R. Soc. London, Ser. A*, 1991, **337**, 291.
- A. Milik, P. Szmolyan, H. Löffelmann and E. Gröller, *International Journal of Bifurcation and Chaos [In Applied Sciences and Engineering]*, 1998, **8**, 505.
- N. Popovic, *J. Phys.: Conf. Ser.*, 2008, **138**, 012020.
- M. Mikikian, M. Cavarroc, L. Couédel, Y. Tessier and L. Boufendi, *Phys. Rev. Lett.*, 2008, **100**, 225005.
- M. Bröns, T. J. Kaper and H. G. Rotstein, *Chaos*, 2008, **18**, 01501.
- M. A. Stern, *J. Reine Angew. Math.*, 1858, **55**, 193.
- A. Brocot, *Revue Chronométrique, Journal des horlogers, Scientifique et Pratique*, 1861, **3**, 186.
- S. B. Guthery, *A Motif of Mathematics: History and Applications of the Mediant and the Farey Sequence*, Docent Press, Boston, 2010.
- R. Graham, D. Knuth and O. Patashnik, *Concrete Mathematics*, Addison–Wesley, 1994, 2nd edn.
- R. Backhouse and J. F. Ferreira, *Science of Computer Programming*, 2011, **76**, 160.
- C. Bonatto and J. A. C. Gallas, *Phys. Rev. Lett.*, 2008, **101**, 054101.
- G. M. Ramirez-Avila and J. A. C. Gallas, *Rev. Boliv. Fis.*, 2008, **14**, 1; G. M. Ramirez-Avila and J. A. C. Gallas, *Phys. Lett. A*, 2010, **375**, 143.
- J. G. Freire and J. A. C. Gallas, *Phys. Rev. E: Stat., Nonlinear, Soft Matter Phys.*, 2010, **82**, 037202.
- For a survey, see: J. A. C. Gallas, *International Journal of Bifurcation and Chaos*, 2010, **20**, 197.
- J. A. C. Gallas, *Observation of discontinuous spirals induced by stable oscillations in a noiseless Duffing proxy*, 2010, submitted for publication.
- J. A. C. Gallas, *Phys. Rev. Lett.*, 1993, **70**, 2714; J. A. C. Gallas, *Appl. Phys. B: Lasers Opt.*, 1995, **60**, S203.
- J. A. C. Gallas, *Phys. A*, 1994, **202**, 196.
- J. A. C. Gallas and H. E. Nusse, *Journal of Economic Behavior & Organization*, 1996, **29**, 447.
- C. Bonatto, J. C. Garreau and J. A. C. Gallas, *Phys. Rev. Lett.*, 2005, **95**, 143905.
- C. Bonatto and J. A. C. Gallas, *Phys. Rev. E: Stat., Nonlinear, Soft Matter Phys.*, 2007, **75**, 055204(R); C. Bonatto and J. A. C. Gallas, *Phil. Trans. R. Soc. London*, 2008, **366A**, 505.
- M. A. Nascimento, J. A. C. Gallas and H. Varela, *Phys. Chem. Chem. Phys.*, 2011, **13**, 441.
- J. G. Freire, K. Showalter and J. A. C. Gallas, in preparation.
- J. G. Freire and J. A. C. Gallas, Stern-Brocot trees in cascades of mixed-mode oscillations and canards in the extended Bonhoeffer-van der Pol and the FitzHugh-Nagumo models of excitable systems, *Phys. Lett. A*, 2011, **375**, 1097.